Polymer 50 (2009) 3319–3328

Contents lists available at ScienceDirect

Polymer

journal homepage: www.elsevier.com/locate/polymer

Effect of tie-layer thickness on the adhesion of ethylene–octene copolymers to polypropylene

A.R. Kamdar [a], R.K. Ayyer [a], B.C. Poon [b], G.R. Marchand [b], A. Hiltner [a,*], E. Baer [a]

[a] Department of Macromolecular Science and Engineering, Center for Applied Polymer Research, Case Western Reserve University, Cleveland, OH 44106-7202, United States
[b] New Products – Materials Science, Core R&D, The Dow Chemical Company, Freeport, TX 77541, United States

ARTICLE INFO

Article history:
Received 2 February 2009
Received in revised form
14 April 2009
Accepted 17 April 2009
Available online 3 May 2009

Keywords:
Delamination toughness
Adhesion
Ethylene-octene copolymers

ABSTRACT

The adhesion of some ethylene–octene copolymers to polypropylene (PP) and high density polyethylene (HDPE) was studied in order to evaluate their suitability as compatibilizers for PP/HDPE blends. A one-dimensional model of the compatibilized blend was fabricated by layer-multiplying coextrusion. The microlayered tapes consisted of many alternating layers of PP and HDPE with a thin tie-layer inserted at each interface. The thickness of the tie-layer varied from 0.1 to 15 μm, which included thicknesses comparable to those of the interfacial layer in a compatibilized blend. The delamination toughness was measured in the T-peel test. Generally, delamination toughness decreased as the tie-layer became thinner with a stronger dependence for tie layers thinner than 2 μm. Inspection of the crack-tip damage zone revealed a change from a continuous yielded zone in thicker tie layers to a highly fibrillated zone in thinner tie layers. By treating the damage zone as an Irwin plastic zone, it was demonstrated that a critical stress controlled the delamination toughness. The temperature dependence of the delamination toughness was also measured. A blocky copolymer (OBC) consistently exhibited better adhesion to PP than statistical copolymers (EO). A one-to-one correlation between the delamination toughness and the reported performance of the copolymers as compatibilizers for PP/HDPE blends confirmed the key role of interfacial adhesion in blend compatibilization.

1. Introduction

Compatibilization of polymer mixtures by the addition of another polymer is conceptually an attractive route for generating blends with unique property combinations and for recycling mixed polymer scrap [1]. The most abundant polymers in use world-wide are polypropylene (PP) and polyethylene (PE). Due to their incompatibility, their blends have extremely low tensile elongation and poor toughness. Incompatibility has been attributed to poor interfacial adhesion between the PP and PE phases resulting in fracture during elongation or impact. A variety of copolymers have been investigated as compatibilizers to improve the interfacial adhesion between PP and PE [2–7], including EPDM, EVA, SBS and SEBS. The compatibilized blends show substantial increases in the elongation at break and the impact strength.

Recently, the effect of chain microstructure of ethylene–octene copolymers as compatibilizers for PP/HDPE blends was studied [8,9]. Comparisons were made between statistical copolymers (EO) and a multiblock copolymer (OBC) that was synthesized using The Dow Chemical Company's novel chain shuttling catalyst technology [10,11]. The OBC consisted of crystallizable ethylene–octene blocks with very low comonomer content and high melting temperature, alternating with amorphous ethylene–octene blocks with high comonomer content and low glass transition temperature. As the OBC soft segment was expected to be compatible with PP and the hard segment was expected to be compatible with HDPE, it was anticipated that OBC would be an excellent compatibilizer for PP/HDPE blends. In the blends, the copolymers were preferentially located at the interface between PP and HDPE where they effectively reduced the interfacial tension and improved the interfacial adhesion. As a result, all the compatibilized blends were ductile. However, the OBC provided higher elongation at break and greater toughness than the statistical EO copolymers [8,9].

Interfacial properties are not easily examined in the dispersed domain morphology of conventional melt blends. An alternative approach takes advantage of layer-multiplying coextrusion to fabricate tapes that consist of many alternating layers of PP and HDPE with individual layer thicknesses on the micron size scale [12]. Insertion of a thin tie-layer at each interface creates a one-dimensional model of the compatibilized blend [13]. A recent study

* Corresponding author.
E-mail address: ahiltner@case.edu (A. Hiltner).

0032-3861/$ – see front matter © 2009 Elsevier Ltd. All rights reserved.
doi:10.1016/j.polymer.2009.04.048

Table 1
Materials.

Material	Designation	C_8 content[a] (mol%)	Density (g/cm^3)	M_w[a] (kg/mol)	M_w/M_n[a]
Isotactic polypropylene	PP		0.900	340	4.6
High density polyethylene	HDPE		0.961	120	9.6
Ethylene–octene statistical copolymer	EO855	17	0.855	130	2.2
Ethylene–octene statistical copolymer	EO876	11	0.876	83	2.0
Ethylene–octene block copolymer	OBC	11	0.880	120	2.8

[a] Data provided by The Dow Chemical Company.

of the adhesion of OBC and two statistical EO copolymers to PP and HDPE using microlayered coextruded tapes found that the OBC exhibited much higher delamination toughness compared to the statistical EO copolymers [14]. This study utilized tie layers with thickness in the range of 2–14 μm, which was considerably thicker than the typical interfacial layer in compatibilized blends, which varied from 0.1 to 0.6 μm [9].

The present study employs microlayered tapes and extends the previous investigation to include tie layers of the nanometer thickness observed in compatibilized blends. The crack-tip damage zone is observed *in situ* and is analyzed in terms of a critical delamination stress for interfacial failure. Additionally, the effect of temperature on the delamination toughness is reported.

2. Materials and methods

The adherends and the tie layers used in this study were provided by The Dow Chemical Company and are tabulated in Table 1. The adherends were an isotactic polypropylene (PP) and a high density polyethylene (HDPE). The tie layers were two statistical ethylene–octene copolymers that differed in the comonomer content (EO855 and EO876), and an ethylene–octene multiblock copolymer (OBC) (Dow Experimental OBC). The EO855 had the same density as the OBC soft segment and the EO876 had approximately the same overall comonomer content and density as the OBC. The schematic structures for these copolymers are described in Scheme 1. All the copolymers had about the same molecular weight, Table 1. The molecular weight, molecular weight distribution, comonomer content, and hard segment content data were provided by Dow.

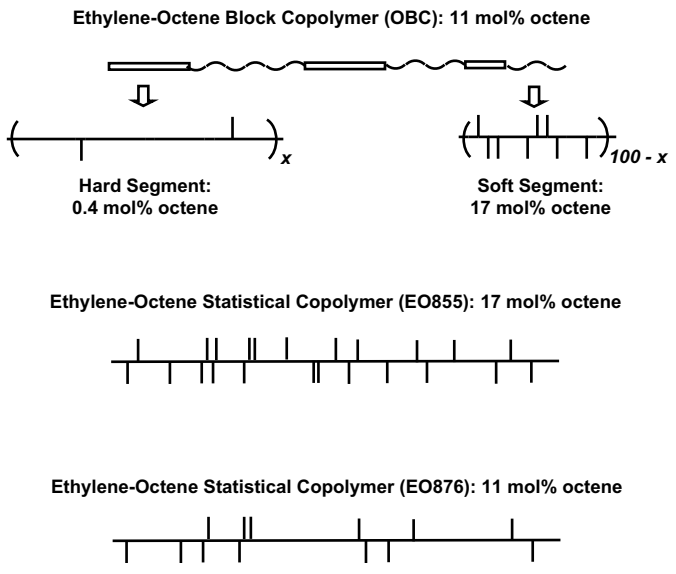

Scheme 1. Schematic representations of the ethylene–octene copolymer tie layers.

Compression molded sheets with thickness of approximately 0.5 mm were prepared for thermal analysis and dynamic mechanical analysis. Pellets were sandwiched between Mylar® sheets, preheated at 190 °C under minimal pressure for 8 min, compressed at 10 MPa for 5 min in a laboratory press, and cooled at about 30 °C/min with circulating cold water. Thermal analysis was performed with a Perkin–Elmer DSC-7 calorimeter under a nitrogen atmosphere. Specimens weighing 5–10 mg were cut from the molded sheets, and thermograms were obtained using a heating/cooling rate of 10 °C/min from −60 to 190 °C. Dynamic mechanical thermal analysis (DMTA) was carried out with a Q800 Dynamic Mechanical Analyzer from TA Instruments. Specimens were tested in the dynamic tensile mode with a frequency of 1 Hz and a strain of 0.1% from −60 to 120 °C with a heating rate of 3 °C/min and a grip to grip separation of 13 mm. The DSC thermograms and DMTA spectra for EO855, EO876 and OBC were published previously [14]. The thermal properties of the copolymers are summarized in Table 2.

The temperature dependence of the yield stress and modulus of the tie-layer materials was measured with ASTM D1708 microtensile specimens cut from the compression molded films. The tests were performed in an MTS Alliance RT/30 testing machine with an environmental chamber cooled with liquid nitrogen. The separation of the grips was 22.3 mm and the specimen width was 4.8 mm. Specimens were stretched at a strain rate of 500%/min at temperatures between −60 to 80 °C. Engineering stress and strain were calculated conventionally from the initial cross-section area and grip separation. The yield stress was determined from the intersection of two tangent lines.

Microlayer tapes were coextruded using the three-component layer-multiplying process described previously [15]. The tapes consisted of alternating layers of polypropylene (PP) and high density polyethylene (HDPE) separated by a thin tie-layer. Microlayered tapes with 65 layers (16 PP layers and 17 HDPE layers separated by 32 layers of the ethylene–octene tie-layer) were coextruded to produce tie-layer thicknesses ranging from 2 to 15 μm [14]. Very thin tie layers ranging from 0.1 to 2 μm were produced using 257 layers (64 PP layers and 65 HDPE layers separated by 128 tie layers). The tapes were about 2 mm thick and 12 mm wide. Different tie-layer thicknesses were produced by varying the extruder feed ratios. The adherend PP and HDPE layers had thickness of about 50 μm for microlayered tapes having 65 layers and about 15 μm for tapes having 257 layers. A microlayered tape of PP and HDPE with no tie-layer was also produced as a control. All the tapes were collected on a conveyor-belt take-off unit and quenched in cold water.

The microlayered tapes were microtomed at −85 °C through the thickness direction and normal to the extrusion direction to expose a cross-section of the layered assembly. The layer uniformity and tie-layer thickness for the center adhesive layer were determined by imaging the microtomed cross-sections with a Digital Laboratories Nanoscope IIIa atomic force microscope (AFM) operating in the tapping mode.

Delamination was carried out with a modified T-peel test (ASTM D1876). Strips 6.4 mm wide and 20 cm long were cut from the center of the microlayered tape and notched by pushing a fresh

Table 2
Selected thermal properties.[a]

Material	ΔH (J/g)	X_c (%)	T_m (°C)	T_c (°C)	T_g (°C)	T_α (°C)
PP	103	50	165	123	18	
HDPE	223	77	137	114		
EO855	9	3	~38	45	−39	–
EO876	37	13	~64	44	−32	–
OBC	39	13	123	98	−42	76

[a] Data from Reference [14].

razor blade into a tie-layer at the mid-plane of the tape. The notch was examined with an optical microscope to ensure that the crack started along a single interface. Tapes were subsequently loaded at 21 °C in the MTS testing machine at a rate of 10 mm/min. The results of 3 tests are reported. The effect of peel temperature on delamination toughness was studied for two tie-layer thicknesses, 0.4 μm and 4 μm. Specimens were peeled at temperatures between −60 and 90 °C at a rate of 10 mm/min in the Instron environmental chamber cooled with liquid nitrogen. Tapes were held at the target temperature for 20 min after reaching equilibrium. At least three specimens of each composition were tested at each temperature.

The composition of the matching peel surfaces was determined by a Nicolet 800 FTIR spectrometer in the ATR mode. Five different areas on each peel surface were tested.

To study the damage zone ahead of the crack tip during delamination, some peel specimens were polished and coated on the edges with 150 Å of gold before being loaded into a tensile deformation stage and inserted into a JEOL 840-A scanning electron microscope (SEM). The specimens were peeled *in situ* at a rate of 0.2 mm/min.

3. Results and discussion

3.1. Delamination toughness of microlayered tapes

The cross-section AFM micrographs revealed the layered structure of the microlayered tapes. Continuous tie layers were successfully coextruded with thicknesses that ranged from 0.1 μm to 14 μm. Examples of EO855 tie layers are shown in Fig. 1a–f. The clearly visible tie layers appeared darker because they had a lower modulus than HDPE and PP. The interfaces between the tie-layer and PP layer and between the tie-layer and HDPE were sharp and undulated. The undulating periodicity along the PP/EO855 interface was attributed to the boundaries of the PP spherulites. In addition, there were more acute interdigitated features. These arose from the influx of tie-layer material into the interstices of PP spherulites during crystallization of the latter [14,16]. The lamellae in the EO855 layer, Fig. 1e,f, were thought to be HDPE fractions that diffused into the tie-layer during melt processing.

The failure location was identified from the composition of the peeled surfaces using the ATR-FTIR. The adherends and adhesive tie layers had unique FTIR peaks that allowed for their differentiation. For the tapes with EO855 as the tie-layer, the spectrum from one surface closely matched that of EO855, Fig. 2a, and the spectrum from the other surface closely matched that of PP, Fig. 2b. Similarly, for the tapes with OBC as the tie-layer, the spectrum from one surface closely matched that of OBC, Fig. 2c, and the spectrum from the other surface closely matched that of PP, Fig. 2d. These observations confirmed that delamination occurred adhesively at the PP/tie-layer interface. A trace of HDPE in the spectra of the tie-layer surface was attributed to diffusion of low molecular weight HDPE fractions into the tie-layer.

When the notched specimen was loaded, the arms bent into the T-peel configuration as the load gradually increased until the crack propagated steadily at a constant load. The beam arms did not return to their original shape upon removal of the load due to some plastic deformation of the beam arms. The delamination toughness G was obtained from the constant load P measured during crack propagation and the specimen width W.

$$G = \frac{2P}{W} \tag{1}$$

The effect of tie-layer thickness on the delamination toughness measured at 21 °C is shown in Fig. 3a. The delamination toughness of the OBC tie-layer was substantially higher than that of the EO855 tie layer, which had the same composition as the OBC soft segment. The delamination toughness of the OBC tie-layer was also substantially higher than that of the EO876 tie-layer, which had the same comonomer content and crystallinity as the OBC. The blocky nature of the OBC was responsible for the higher delamination toughness compared to the two statistical copolymers. The results reproduced the linear relationship between G and tie-layer thickness that was reported previously for tie layers 2 μm and thicker [14]. However, the linear relationship did not extend to tie layers thinner than 2 μm. Instead, G showed a stronger dependence on tie-layer thickness that extrapolated to the low value of G for the microlayered tape of PP and HDPE with no tie-layer.

Based on these observations, two regimes in tie-layer thickness were defined: a thick tie-layer regime with tie layers between 2 and 14 μm and a thin tie-layer regime with tie layers less than 2 μm. In the thick tie-layer regime, the delamination toughness of OBC and EO855 tie layers increased linearly with the tie-layer thickness, indicating that energy was absorbed by uniform deformation of the entire tie-layer thickness. For thick EO876 tie layers, the delamination toughness was independent of the tie-layer thickness. In this case, it was likely that the entire tie-layer did not deform uniformly; rather, the deformation was limited to a small, localized region of the tie-layer at the PP interface that did not depend on the tie-layer thickness. In the thin tie-layer regime, a stronger linear dependence of delamination toughness on the tie-layer thickness was observed for all the tie layers, as shown for clarity in the enlarged plot in Fig. 3b.

3.2. Delamination mechanism

The damage zone at the crack tip of the EO855 tie-layer is shown in Fig. 4 for tie layers of several thicknesses. A well-defined and continuous yielded zone was observed in the thicker tie layers, as exemplified by tie-layer thicknesses of 10 μm and 4 μm in Fig. 4a, b respectively. The damage zone length and the crack-tip opening decreased as the tie-layer thickness decreased, which was consistent with deformation of the entire tie-layer thickness. As the tie-layer thickness was reduced further, the crack-tip opening and damage zone length were significantly smaller, as illustrated with tie-layer thicknesses of 0.8 μm and 0.2 μm in Fig. 4c,d. Higher magnifications of the damage zones of the thin tie layers revealed a highly fibrillated craze zone with nearly 60–70% void spacing between the load-bearing fibrils, Fig. 4e,f.

The damage zones for EO876 tie layers are shown in Fig. 5. The thick 10 μm and 4 μm tie layers formed a continuous, yielded zone, Fig. 5a, b. However comparison with the thick EO855 tie layers revealed that the damage zone was much smaller in the EO876 tie layers. This was evident in both the length of the damage zone and the crack-tip opening. Moreover, in contrast to the EO855 tie layers, the damage zone length did not depend strongly on the tie-layer thickness, which was consistent with localized deformation of the tie-layer at the PP/tie-layer interface. For thin EO876 tie layers, the damage zone was fibrillated with significant voiding as in EO855, Fig. 5c,d. Higher magnification of the damage zones revealed the highly fibrillated craze morphology, Fig. 5e,f.

The thick OBC tie layers formed a continuous, yielded zone at the crack tip that was shorter than the damage zone in thick EO855 tie layers, Fig. 6a,b. The thin OBC tie layers showed a highly fibrillated damage zone with considerable voiding, Fig. 6c–f, as was observed with thin EO855 and EO876 tie layers.

The two types of damage zones shown schematically in Fig. 7 corresponded to the two regimes in the delamination toughness (see Fig. 3). Thick tie layers, i.e. those between 2 and 14 μm, exhibited a continuous yielded zone. In this regime, it appeared

that the entire OBC and EO855 tie layers yielded to form the damage zone, whereas the EO876 tie-layer yielded locally at the PP interface. In contrast to the thick tie layers, the thin tie layers, i.e. those thinner than 2 μm, exhibited a highly voided and fibrillated damage zone. Apparently, when the tie-layer was thinner than 2 μm, it did not contain enough material to support a continuous yielded zone and voids formed in the damage zone as the tie-layer was stretched. Moreover, the presence of influxes might have affected delamination of thin tie layers more than thick tie layers, thereby reducing the differences among the various tie-layer materials.

3.3. Damage zone analysis

Three factors contribute to the delamination toughness: tie-layer deformation, beam arm deformation, and interfacial adhesive failure. The beam arm deformation consists of two components: stretching and bending. In similar peel tests using microlayered tapes, both contributions were found to be within the experimental error [17], and could be neglected. The adhesive contribution is reflected in the extrapolated value of delamination toughness. Although G of the interface between PP and HDPE is larger than theoretically predicted due to the presence of influxes [18], it is

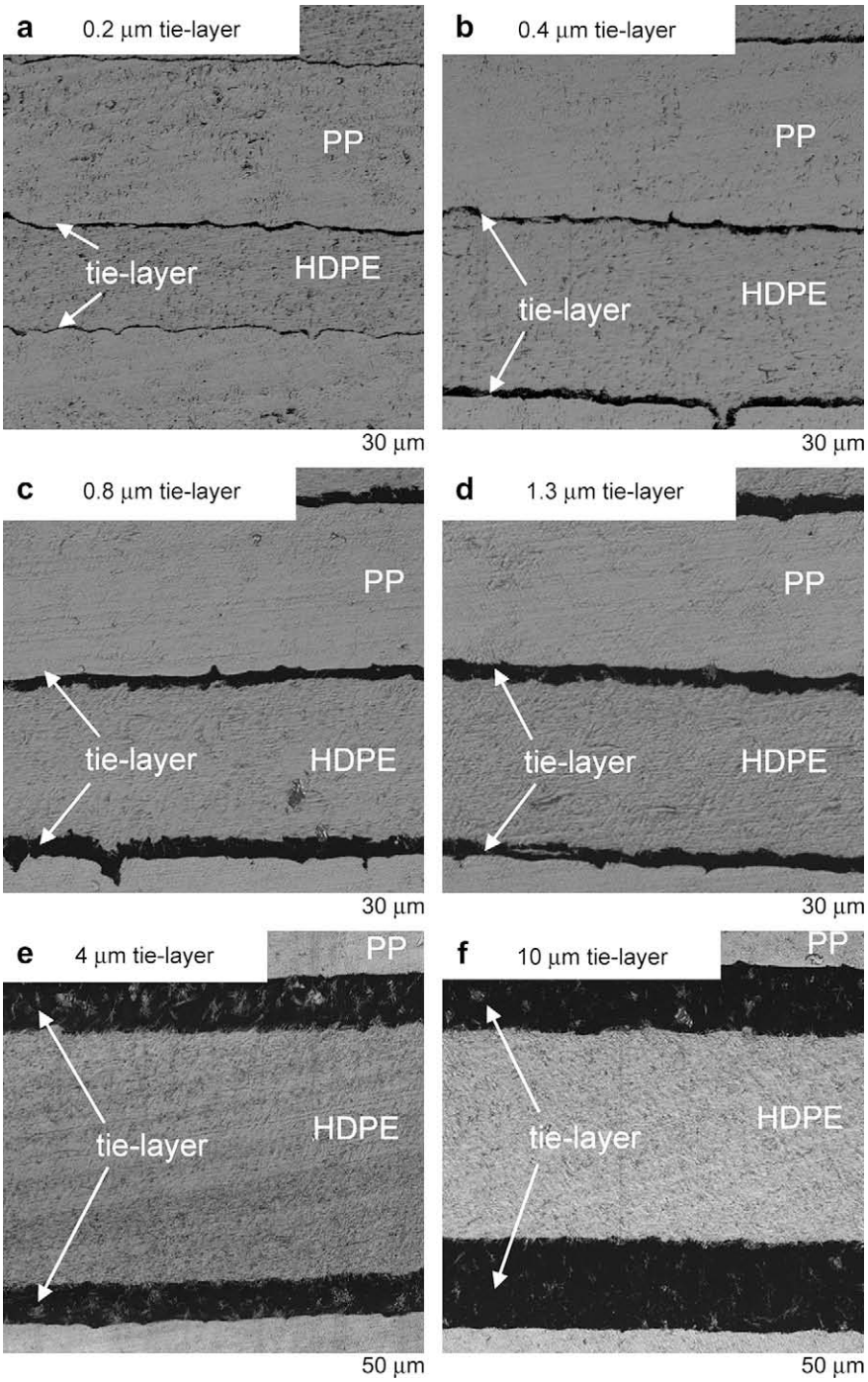

Fig. 1. AFM phase images of the microlayer tape cross-sections showing the layered structure of tapes with different EO855 tie-layer thicknesses. (a) 0.2 μm; (b) 0.4 μm; (c) 0.8 μm; (d) 1.3 μm; (e) 4 μm; (f) 10 μm.

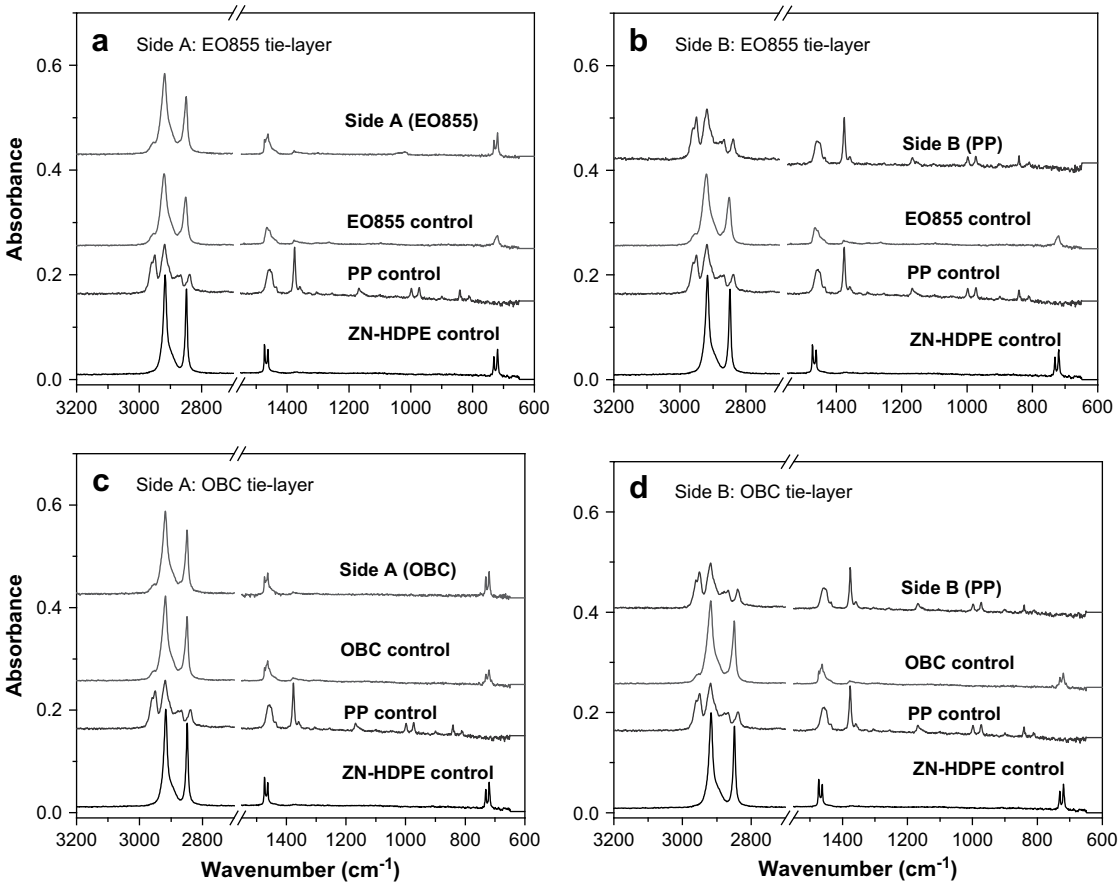

Fig. 2. Identification of matching peel fracture surfaces using ATR-FTIR. (a) and (b) The matching peel surfaces A and B from a tape with 0.4 μm EO855 tie layers; and (c) and (d) the matching peel surfaces A and B from a tape with 0.4 μm OBC tie layers. The spectra of the tape constituents are included for comparison.

nevertheless small compared to G when a tie-layer is inserted between PP and HDPE. Rather, the influxes at the interface between PP and a soft tie-layer provide connectivity to support the stress required for yielding of the tie-layer. In the following analysis, it is assumed that G is determined primarily by viscoelastic–plastic deformation of the tie-layer. Therefore, the delamination toughness was analyzed by considering the damage zone as an Irwin plastic zone. Assuming that only the tie-layer undergoes plastic

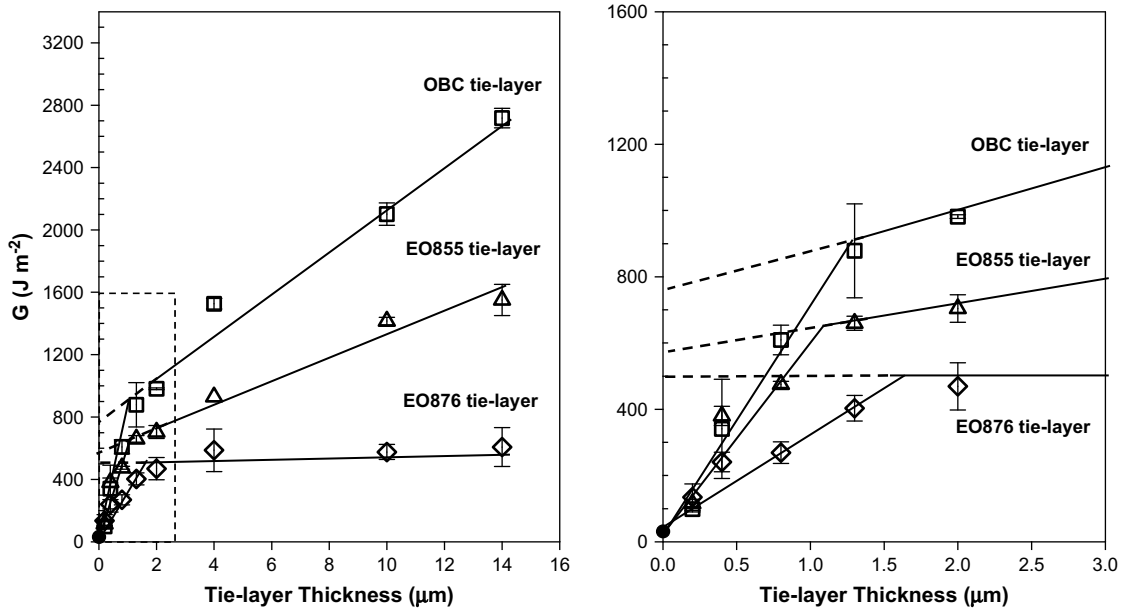

Fig. 3. Effect of tie-layer thickness on the delamination toughness. (a) The entire range of tie-layer thicknesses studied; and (b) a magnified plot of the results for thinner tie layers. The crosshead speed was 10 mm/min and the temperature was 21 °C.

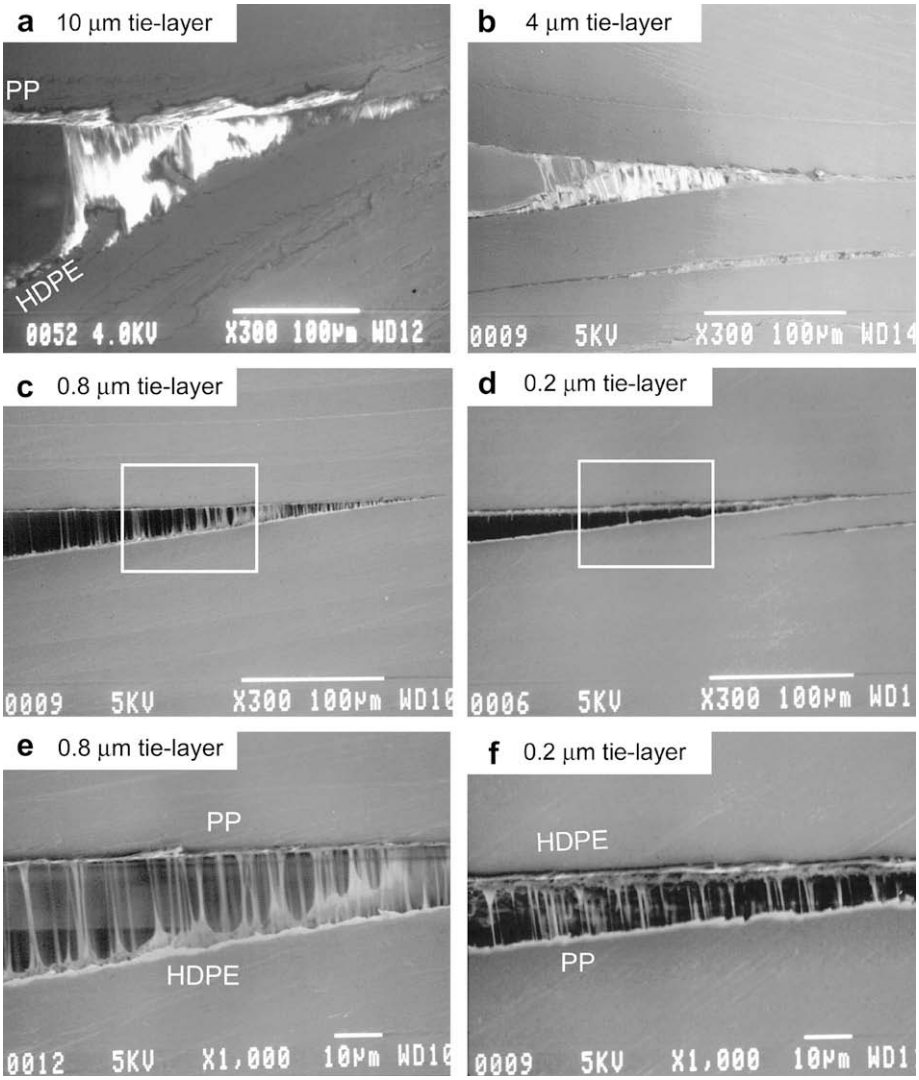

Fig. 4. SEM images from an *in-situ* peel test showing the crack-tip damage zone for EO855 tie layers of different thicknesses: (a) 10 μm; (b) 4 μm; (c) 0.8 μm; (d) 0.2 μm; (e) 0.8 μm (1000×); and (f) 0.2 μm (1000×).

deformation with formation of a localized yielded zone of length a at the crack tip, the delamination toughness is given as [19,20]

$$G_p = \frac{2\pi a \sigma_y^2}{E} \tag{2}$$

The yield stress σ_y and the modulus E of the tie-layer were taken from constrained uniaxial tensile tests that simulated the deformation of tie layers in the peel test, Fig. 8. The initial response reflected the amount of crystallinity. Thus, OBC and EO876 had about the same modulus and yield stress, whereas the values for EO855 were much lower. The yield stress of OBC, EO876 and EO855 was 2.4, 2.5 and 1 MPa, respectively, and the secant modulus values at 5% strain were 16, 9.1 and 1.6 MPa, respectively. The difference between the statistical and blocky copolymers appeared at higher strains. Neither EO876 nor EO855 exhibited strong strain hardening, whereas pronounced strain hardening of OBC resulted in a higher fracture stress. The difference in the high strain response arose from the differences in the crystalline entities of statistical and blocky copolymers [21]. During stretching of EOs, melting of fringed micellar crystals and recrystallization as oriented micellar crystals did not impart a substantial increase in the tensile strength. However, in OBC, irreversible deformation of crystalline lamellae followed by fibrillation produced the strong strain hardening [22,23].

The values of G_p from Eq. (2) are compared with the experimental values of G obtained in the T-peel test for the EO855 tie layers in Table 3. In the thick tie-layer regime, G_p was comparable to G within 10–15%. In the thin tie-layer regime, G_p obtained from the measured damage zone length a was much larger than G. However, the damage zone in the thin tie layers was highly voided, and only the fibrils were load-bearing. Hence, a was replaced with an effective damage zone length a_f which considered only the fraction of the damage zone length supported by fibrils. Then

$$G_{pf} = \frac{2\pi a_f \sigma_y^2}{E} \tag{3}$$

where a_f was obtained by subtracting the voided length from the total damage zone length. The resulting G_{pf} agreed well with the measured G to within 15%, Table 3.

Comparable calculations for EO876 tie layers also gave good agreement between G_p or G_{pf} and G, Table 4. In the thick tie-layer regime, a and G were essentially independent of the tie-layer thickness, which was consistent with localized yielding at the PP/tie-layer

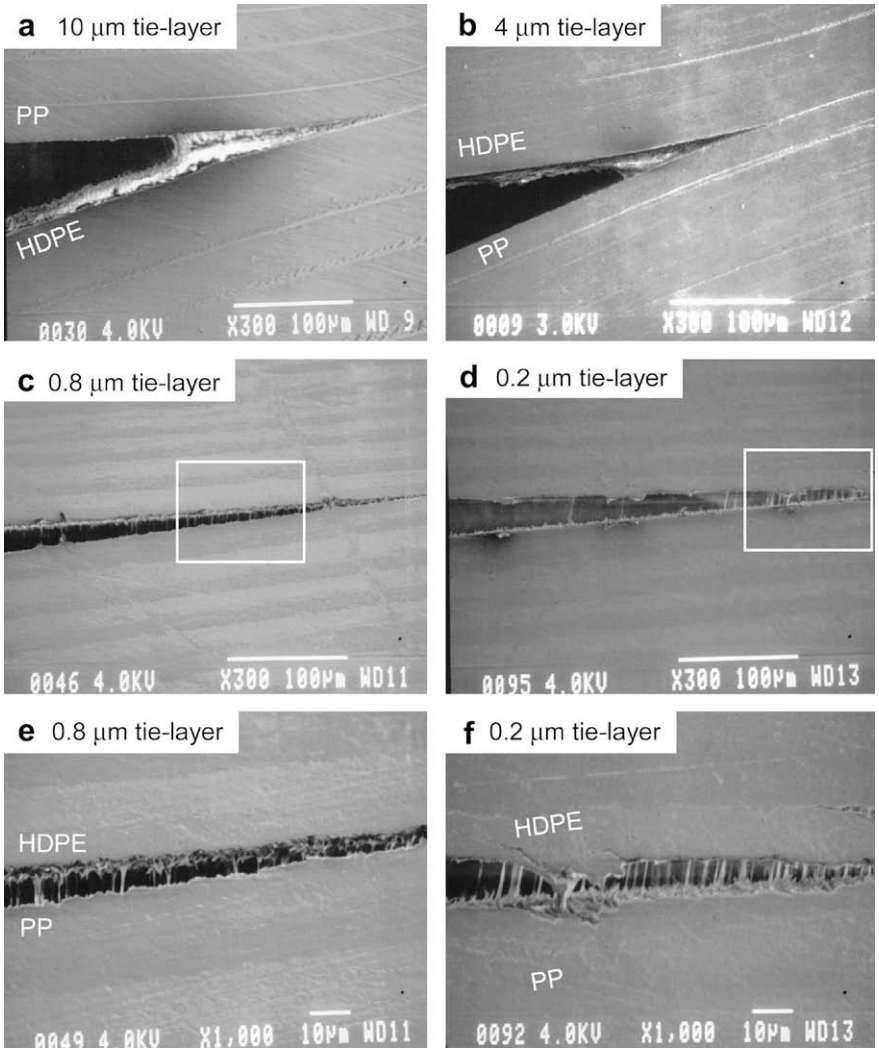

Fig. 5. SEM images from an *in-situ* peel test showing the crack-tip damage zone for EO876 tie layers of different thicknesses: (a) 10 μm; (b) 4 μm; (c) 0.8 μm; (d) 0.2 μm; (e) 0.8 μm (1000×); and (f) 0.2 μm (1000×).

interface. The value of G_p from Eq. (2) was comparable to the measured G within 25%, Table 4. In the thin tie-layer regime, there were fewer fibrils than in EO855. The delamination toughness calculated from Eq. (3) was in good agreement with the measured delamination toughness.

A similar analysis of the OBC tie layers using the measured yield stress resulted in G_p that substantially under-estimated the measured G. It was noted from the stress–strain curves in Fig. 8 that OBC underwent pronounced strain hardening in contrast to EO855 and EO876. This suggested that the delamination in OBC was controlled by a critical delamination stress σ_c that exceeded σ_y. To obtain σ_c, Eq. (2) was rewritten as

$$\sigma_c = \left(\frac{GE}{2\pi a}\right)^{1/2} \tag{4}$$

It was observed that in both thin and thick tie-layer regimes, the critical delamination stress values calculated from Eq. (4) fell in the strain-hardening region of the OBC stress–strain curve, Table 5. In the thick tie-layer regime, σ_c was essentially independent of the tie-layer thickness with a value of about 5 MPa. The values of σ_c in the thin tie-layer regime were significantly higher. Possibly the unconstrained fibrils in the voided damage zone were able to support higher stresses and strains than the yielded material of constrained damage zone.

The critical stress approach for OBC tie-layer was tested by comparing the corresponding critical draw ratio λ_c with the maximum draw ratio in the damage zone λ_{max}. The critical strain ε_c corresponding to σ_c was obtained from the stress–strain curves and the critical draw ratio was calculated according to

$$\lambda_c = \frac{\varepsilon_c}{100} + 1 \tag{5}$$

The maximum draw ratio in the damage zone was defined as

$$\lambda_{max} = \frac{d}{d_0} \tag{6}$$

where d is the maximum crack-tip opening and d_0 is the initial tie-layer thickness. It was observed that for the thick tie layers λ_c and λ_{max} were in good agreement within 30%, Table 5. However, for the thinnest tie layers, the maximum draw ratio in the damage zone exceeded the fracture strain of OBC. This was additional evidence that the unconstrained fibrils of the voided damage zone exhibited a different stress–strain relationship from the yielded material of the constrained damage zone. Nevertheless, it appeared that the delamination toughness of OBC followed a critical stress condition, rather than a yield stress condition, regardless of the tie-layer thickness.

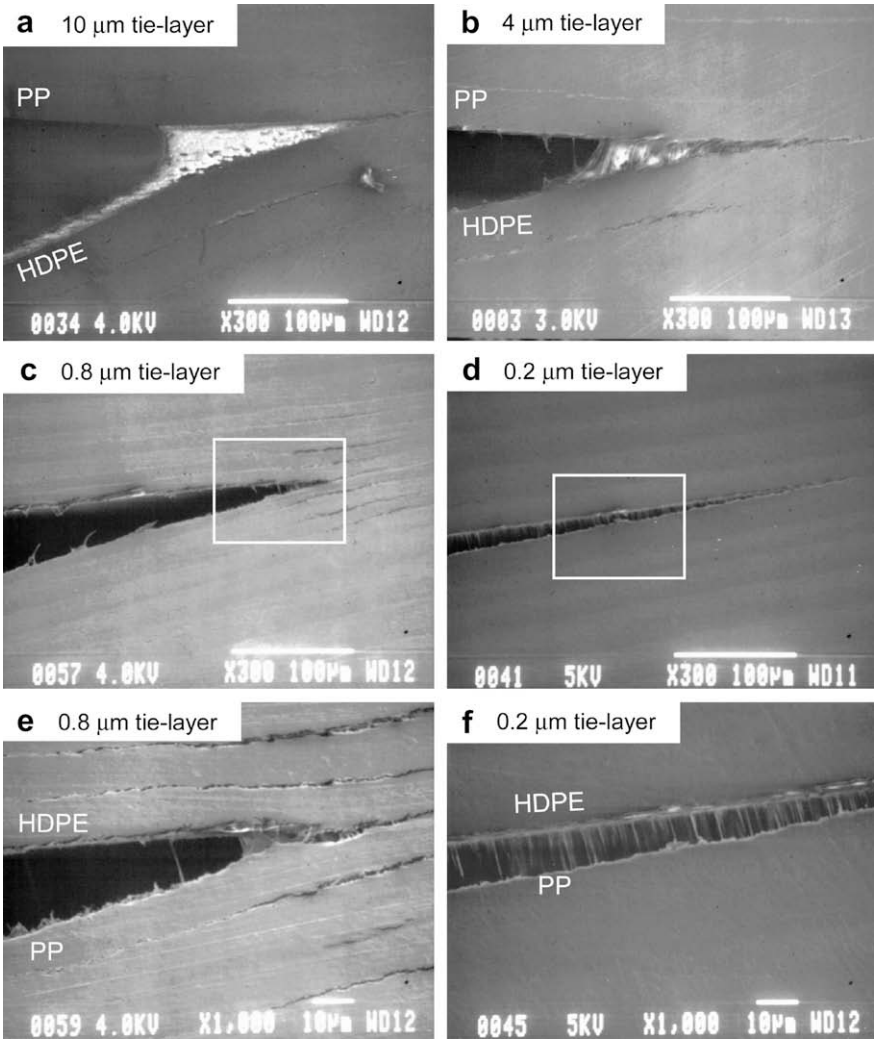

Fig. 6. SEM images from an *in-situ* peel test showing the crack-tip damage zone for OBC tie layers of different thicknesses: (a) 10 μm; (b) 4 μm; (c) 0.8 μm; (d) 0.2 μm; (e) 0.8 μm (1000×); and (f) 0.2 μm (1000×).

3.4. Effect of temperature on the delamination toughness

The effect of temperature on the delamination toughness was measured for the thick and thin tie layers at a peel rate of 10 mm/min. The results for tie layers having thicknesses of 4 μm and 0.4 μm are shown in Fig. 9a, b, respectively. A maximum in the delamination toughness was observed for each of the tie layers near the tie-layer T_g. Below the T_g, failure occurred before the beam arms were able to bend into the T-peel configuration irrespective of the tie-layer thickness. The PP/tie-layer interface failed catastrophically without achieving stable crack propagation. Above the T_g, the

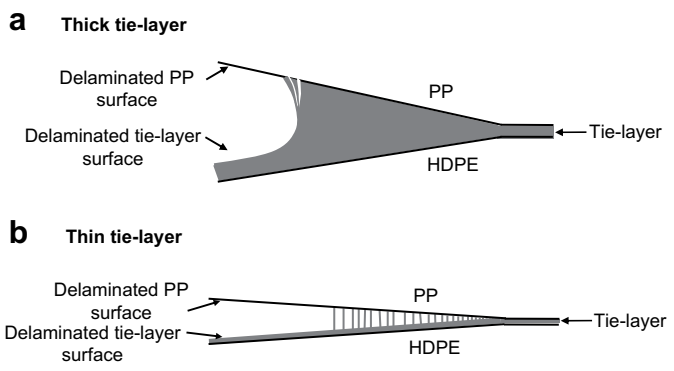

Fig. 7. Schematic representation of the tie-layer damage zone. (a) Thick tie layers (2–14 μm); and (b) thin tie layers (less than 2 μm).

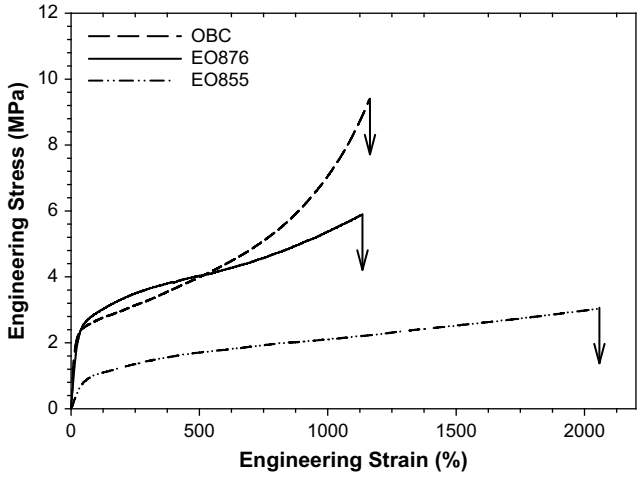

Fig. 8. Constrained stress–strain curves of the tie-layer copolymers [14].

Table 3
Comparison of the measured delamination toughness of EO855 tie layers with the delamination toughness calculated from the yield stress.

Tie-layer thickness l_o (μm)	Damage zone length a (μm)	Effective damage zone length a_f (μm)	Calculated delamination toughness G_p (J/m^2)	Calculated delamination toughness G_{pf} (J/m^2)	Measured delamination toughness G (J/m^2)
0.2	140	33	–	143	120 ± 10
0.4	226	100	–	430	430 ± 30
0.8	244	125	–	540	530 ± 10
1.3	120	112	–	440	660 ± 20
2	196	–	728	–	700 ± 40
4	207	–	895	–	930 ± 10
10	272	–	1180	–	1410 ± 20
14	362	–	1421	–	1550 ± 100

delamination toughness decreased as the temperature increased. The OBC exhibited higher G than EO855 and EO876 over the temperature range of −20 °C to 60 °C. At higher temperatures, a drop in G to almost zero over a small change in temperature was clearly evident in the 4 μm tie layers, Fig. 9a. The transition temperature occurred at 40–50 °C for EO855, 60–70 °C for EO876 and 70–80 °C for OBC. The transition temperature corresponded to the T_m of EO855 ($T_m = 38$ °C) and of EO876 ($T_m = 64$ °C) and to the T_α of OBC ($T_\alpha = 76$ °C). Above the transition temperature, failure occurred cohesively through the tie-layer due to softening of the crystalline phase. The 0.4 μm tie layers exhibited lower G than the 4 μm tie layers at all temperatures, Fig. 9b. The thinner tie layers also exhibited a maximum in G near the T_g, however the higher temperature transition was not clearly evident.

A decrease in delamination toughness with increasing temperature is often observed [17,24]. According to Eq. (2), the temperature dependence of G can be understood from the change in the modulus and yield stress. The effect of temperature on the yield stress is shown in Fig. 10. As expected, the yield stress of OBC and EO876 was comparable whereas that of EO855 was consistently lower at all the temperatures studied. Qualitatively, the temperature dependence

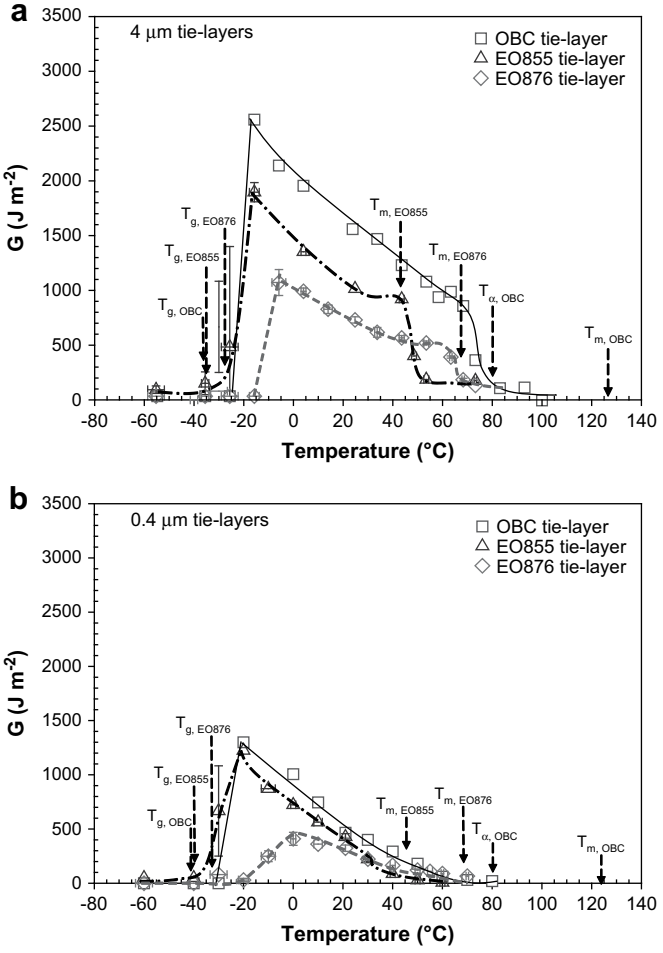

Fig. 9. Effect of temperature on the delamination toughness: (a) 4 μm tie layers; and (b) 0.4 μm tie layers.

Table 4
Comparison of the measured delamination toughness of EO876 tie layers with the delamination toughness calculated from the yield stress.

Tie-layer thickness l_o (μm)	Damage zone length a (μm)	Effective damage zone length a_f (μm)	Calculated delamination toughness G_p (J/m^2)	Calculated delamination toughness G_{pf} (J/m^2)	Measured delamination toughness G (J/m^2)
0.2	317	18	–	78	140 ± 40
0.4	263	46	–	198	240 ± 30
0.8	353	93	–	401	270 ± 30
1.3	197	78	–	336	400 ± 40
2	143	–	617	–	470 ± 90
4	127	–	548	–	590 ± 50
10	177	–	763	–	580 ± 50
14	171	–	738	–	610 ± 120

of the yield stress paralleled the temperature dependence of G (Fig. 9) including the transitional drop at higher temperatures.

The temperature dependence of G_p was calculated from the yield stress and modulus according to Eq. (2). The temperature dependence of a was not readily obtained and in this calculation a was assumed to be constant. Values of 207 μm for the 4 μm EO855 tie-layer and 127 μm for the 4 μm EO876 tie-layer at 21 °C were chosen for the calculations. Results for EO855 and EO876 are tabulated in Tables 6 and 7. The G_p values were within 30% of G for EO855 and within 20% for EO876. For OBC, G depended on a critical stress rather than the yield stress. Assuming a constant a of 168 μm, the value at 21 °C, σ_c was calculated from G at each temperature. The results in Table 8 show that σ_c exceeded σ_y except at the highest

Table 5
The critical delamination stress and draw ratio for OBC tie layers.

Tie-layer thickness l_o (μm)	Damage zone length a (μm)	Effective damage zone length a_f (μm)	Calculated delamination toughness G_p (J/m^2)	Calculated delamination toughness G_{pf} (J/m^2)	Measured delamination toughness G (J/m^2)	Critical delamination stress σ_c (MPa)	Critical strain ε_c (%)	Critical draw ratio λ_c	Crack-tip opening d (μm)	Maximum draw ratio λ_{max}
0.2	144	8	–	18	100 ± 10	5.6	850	9.5	4	20
0.4	56	14	–	33	340 ± 150	7.7	1060	11.6	10	25
0.8	46	31	–	70	610 ± 40	7.1	1000	11.0	10	12.5
1.3	40	33	–	75	880 ± 140	8.2	1090	11.9	15	11.5
2	94	–	200	–	980 ± 5	5.3	780	8.8	18	8.3
4	168	–	360	–	1530 ± 30	4.9	720	8.2	33	7.4
10	233	–	475	–	2100 ± 70	5.0	730	8.3	68	6.5
14	306	–	690	–	2720 ± 60	4.8	690	7.9	113	7.8

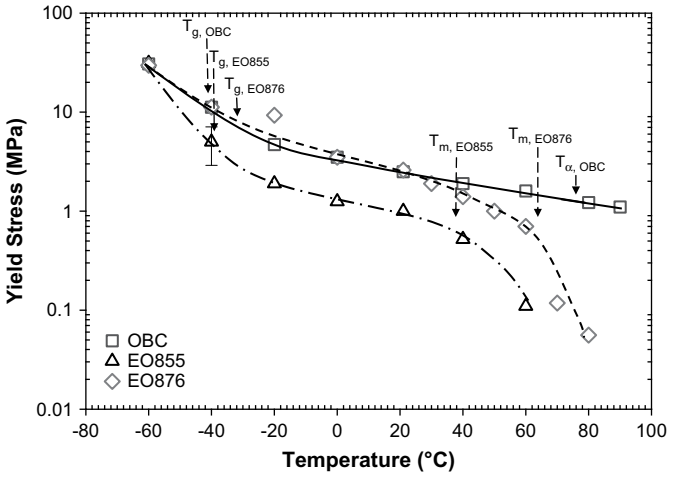

Fig. 10. Effect of temperature on the yield stress of the tie-layer copolymers.

Table 6
Effect of temperature on the delamination toughness of 4 μm EO855 tie layers.

Temperature (°C)	Yield stress σ_y (MPa)	5% Secant modulus E (MPa)	Calculated delamination toughness G_p (J/m^2)	Measured delamination toughness G (J/m^2)
−20	1.9	3.0	1565	1880 ± 90
0	1.25	2.16	941	1330 ± 50
21	1.0	1.60	813	990 ± 10
40	0.52	0.46	765	900 ± 20

temperature, however σ_c gradually decreased as the temperature was raised paralleling the changes in modulus and yield stress.

It is now possible to correlate the adhesion measured with microlayered tapes in this study with the performance of the same copolymers as compatibilizers for PP/HDPE (70/30 wt/wt) blends reported previously [9]. The same ranking of the copolymers was obtained in both studies with OBC imparting both the strongest adhesion in microlayered tapes and the highest tensile toughness in blends. Similarly, EO876 showed the poorest performance in both studies. In terms of the temperature dependence, the abrupt drop in adhesion at the copolymer T_g correlated with the brittle-to-ductile transition in blends. The one-to-one correlation confirms the key role of interfacial adhesion in the performance of compatibilized blends.

Table 7
Effect of temperature on the delamination toughness of 4 μm EO876 tie layers.

Temperature (°C)	Yield stress σ_y (MPa)	5% Secant modulus E (MPa)	Calculated delamination toughness G_p (J/m^2)	Measured delamination toughness G (J/m^2)
0	3.4	10.5	698	880 ± 30
21	2.6	9.1	704	590 ± 30
30	1.9	5.7	590	510 ± 50
40	1.4	3.2	538	480 ± 20

Table 8
Effect of temperature on the critical delamination stress of 4 μm OBC tie layers.

Temperature (°C)	Yield stress σ_y (MPa)	5% Secant modulus E (MPa)	Measured delamination toughness G (J/m^2)	Critical delamination stress σ_c (MPa)
−20	4.7	26.1	2550 ± 60	8.0
0	3.5	19.9	1940 ± 30	6.1
21	2.4	16.0	1530 ± 30	4.9
40	1.9	11.3	1210 ± 20	3.6
60	1.6	9.4	960 ± 60	2.9
80	1.2	6.0	70 ± 10	0.6

4. Conclusions

This study examined the effect of chain microstructure on the adhesion of some ethylene–octene copolymers to PP and HDPE in order to evaluate their suitability as compatibilizers for PP/HDPE blends. In microlayered tapes, all the delamination failures occurred at the PP–copolymer interface, indicating that the copolymers exhibited better adhesion to HDPE than to PP. The blocky OBC copolymer consistently exhibited better adhesion to PP, measured as the delamination toughness, than the statistical EO copolymers. A statistical EO copolymer with higher comonomer content exhibited better adhesion to PP than a statistical EO copolymer with lower comonomer content. The delamination toughness correlated well with the reported performance of the copolymers as compatibilizers for PP/HDPE blends. For all the tie layers, the dependence of delamination toughness on the tie-layer thickness was stronger in thin tie layers, i.e. those less than 2 μm thick, than in thicker tie layers. Inspection of the crack-tip damage zone revealed that a change from a continuous plastic damage zone in thicker tie layers to a highly fibrillated damage zone in thinner tie layers was responsible. By treating the damage zone as an Irwin plastic zone, it was demonstrated that a critical stress controlled the delamination toughness. For the statistical EO copolymers, this was found to be the yield stress. The OBC exhibited considerably stronger strain hardening than the EO copolymers, and in this case delamination was controlled by a critical stress in the strain-hardening region.

Acknowledgements

The authors thank The Dow Chemical Company for generous technical and financial support. Support for the layer-multiplying coextrusion facility was provided by the NSF Science and Technology Center for Layered Polymer Systems under grant number 0423914.

References

[1] Majumdar B, Paul DR. Reactive processing. In: Paul DR, Bucknall CB, editors. Polymer blends, vol. 1. New York: Wiley; 2000 [chapter 17].
[2] Stehling FC, Huff T, Speed CS, Wissler G. J Appl Polym Sci 1981;26:2693–711.
[3] Bartlett DW, Barlow JW, Paul DR. J Appl Polym Sci 1982;27:2351–60.
[4] Ha CS. J Appl Polym Sci 1989;37:317–34.
[5] Blom HP, Teh JW, Rudin A. J Appl Polym Sci 1996;61:959–68.
[6] Souza AMC, Demarquette NR. Polymer 2002;43:3959–67.
[7] Vranjes N, Rek V. Macromol Symp 2007;258:90–100.
[8] Chen HY, Dias PS, Poon BC, Hiltner A, Baer E. In: ANTEC 2007 society of plastics engineers conference proceedings; 2007. p. 1201–5.
[9] Lin YJ, Yakovleva V, Chen HY, Hiltner A, Baer E. J Appl Polym Sci 2009;113:1945–52.
[10] Arriola DJ, Carnahan EM, Hustad PD, Kuhlman RL, Wenzel TT. Science 2006; 312:714–9.
[11] Shan LPC, Hazlitt LG. Macromol Symp 2007;257:80–93.
[12] Poon BC, Chum SP, Hiltner A, Baer E. Polymer 2004;45:893–903.
[13] Ebeling T, Hiltner A, Baer E. J Appl Polym Sci 1998;68:793–805.
[14] Dias P, Lin YJ, Poon B, Chen HY, Hiltner A, Baer E. Polymer 2008;49:2937–46.
[15] Bernal-Lara TE, Ranade A, Hiltner A, Baer E. Nano- and microlayered polymers: structure and properties. In: Michler GH, Balta Calleja FJ, editors. Mechanical properties of polymers based on nanostructure and morphology. Boca Raton: CRC Press; 2005. p. 629–81.
[16] Bartczk Z, Galeski A. Polymer 1986;27:544–8.
[17] Ronesi V, Cheung YW, Hiltner A, Baer E. J Appl Polym Sci 2003;89:153–62.
[18] Wool RP. Polymer interfaces: structure and strength. New York: Hanser; 1995 [chapter 10].
[19] Dillard DA. Fundamentals of stress transfer in bonded system. In: Dillard DA, Pocius AV, editors. The mechanics of adhesion, adhesion science and engineering, vol. I. Amsterdam: Elsevier; 2002. p. 1–44.
[20] Kinloch AJ, Young RJ. Fracture behavior of polymers. Essex: Applied Science; 1983. p. 74–106.
[21] Wang H, Khariwala DU, Cheung W, Chum SP, Hiltner A, Baer E. Macromolecules 2007;40:2852–62.
[22] Wang HP, Chum SP, Hiltner A, Baer E. J Appl Polym Sci, in press. doi:10.1002/app30070.
[23] Wang HP, Chum SP, Hiltner A, Baer E. J Polym Sci B Polym Phys, in press.
[24] Ebeling T, Hiltner A, Baer E. Polymer 1999;40:1525–36.